

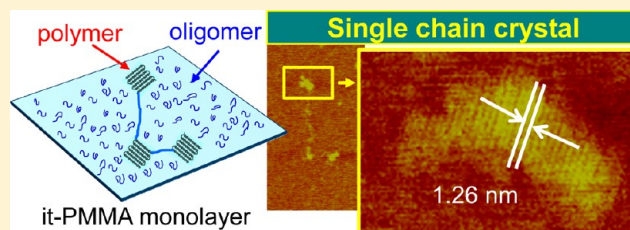
# Crystallization Behavior of Single Isotactic Poly(methyl methacrylate) Chains Visualized by Atomic Force Microscopy

Takahiro Anzai,<sup>†,§</sup> Mariko Kawauchi,<sup>‡</sup> Takehiro Kawauchi,<sup>‡,||</sup> and Jiro Kumaki<sup>\*,†</sup>

<sup>†</sup>Department of Polymer Science and Engineering, Graduate School of Science and Engineering, Yamagata University, Yonezawa, Yamagata 992-8510, Japan

<sup>‡</sup>Department of Environmental and Life Sciences, Toyohashi University of Technology, Tempaku-cho, Toyohashi, Aichi 441-8580, Japan

**ABSTRACT:** We have, for the first time, successfully visualized the crystallization behavior of a single isolated polymer chain at the molecular level by atomic force microscopy (AFM). Previously, we found that isotactic poly(methyl methacrylate) (it-PMMA) formed two-dimensional folded chain crystals composed of double-stranded helices upon compression of its Langmuir monolayer on a water surface, and the molecular images of the crystals deposited on mica were clearly visualized by AFM (Kumaki, J.; et al. *J. Am. Chem. Soc.* **2005**, *127*, 5788). In the present study, a high-molecular-weight it-PMMA was diluted in a monolayer of an it-PMMA oligomer which cannot crystallize at the experimental temperature due to its low molecular weight. At a low surface pressure, isolated amorphous chains of the high-molecular-weight it-PMMA solubilized in the oligomer monolayer were observed. On compression, the isolated chains converted to crystals composed of a single chain, typically some small crystallites linked by an amorphous chain like a necklace. Detailed AFM observations of the crystals indicated that the crystalline nuclei preferentially formed at the ends of the chains, and the size of the nuclei was almost independent of the molecular weight of it-PMMA over a wide range. At an extremely slow compression, crystallization was promoted, resulting in crystallization of the whole chain. The crystallization behavior of a single isolated chain provides new insights in understanding the polymer crystallization process.



## 1. INTRODUCTION

Polymer crystallization is one of the most important issues in polymer science and has been extensively studied for more than 70 years in various experimental and theoretical ways and, recently, by computational simulations.<sup>1–5</sup> However, the crystallization mechanism, especially at a molecular level, is still not well-understood. Crystallization usually involves many polymer chains, which makes the process more complicated. To simplify the system, in the present study, we tried to observe crystallization of a single isolated chain at a molecular level by atomic force microscopy (AFM). If one could directly observe the crystallization of a single chain, new insights into the crystallization mechanism are expected; for example, we may know whether a polymer chain starts crystallization at the end or at the middle of the chain, how a crystalline nuclei forms, and how the chain folds to be a folded-chain crystal. On the basis of the molecular information, we may be able to control the crystallization of polymers in a more sophisticated manner such as by molecular design. However, in conventional three-dimensional (3D) systems, crystallization of a single polymer chain was difficult to observe, since an extremely dilute system is necessary to obtain single-chain crystals avoiding aggregation of multiple chains. Previous workers spread dilute solutions of hydrophobic polymers onto a water surface to obtain single-molecular particles, then annealed to crystallize

them,<sup>6</sup> or freeze-dried dilute polymer solutions to obtain single-molecular crystals.<sup>7</sup> However, by these methods, observation of the crystallization process is not possible.

AFM is a powerful tool to observe materials at a molecular or atomic level, and is commonly used for observation of polymer structures.<sup>8–17</sup> We found that, using 2D samples which are suitable for observation by scanning probe microscopy, various polymer structures could be observed at a resolution close to, or slightly better than, 1 nm using a conventional tapping-mode AFM.<sup>18–33</sup> We used the Langmuir–Blodgett (LB) technique or spin-cast polymer solutions onto substrates to prepare 2D samples, and succeeded to visualize single isolated chains,<sup>18–20</sup> crystals,<sup>21,22</sup> stereocomplexes,<sup>23,24</sup> Langmuir monolayers,<sup>25,26</sup> and helical polymers<sup>27–33</sup> at the molecular level. Among them, we observed an isotactic poly(methyl methacrylate) (it-PMMA) Langmuir monolayer deposited on mica by AFM, and found upon compression that the it-PMMA monolayer crystallized to form 2D folded-chain crystals composed of double-stranded helices.<sup>21</sup> High-resolution AFM successfully visualized the chain packing in the folded-chain crystal, along with chain folding and tie chains at the molecular level for the

**Received:** September 9, 2014

**Revised:** November 14, 2014

**Published:** December 11, 2014

first time.<sup>21</sup> We also observed the melting behavior of this 2D folded-chain crystal in situ at the molecular level by a high-temperature AFM, and found a significant melting point depression by as much as 100 °C occurred due to the two dimensionality of the crystals.<sup>22</sup>

In the present study, we chose it-PMMA Langmuir monolayer in order to prepare and observe a single-chain crystal. The basic idea was simple (Figure 1). A small amount

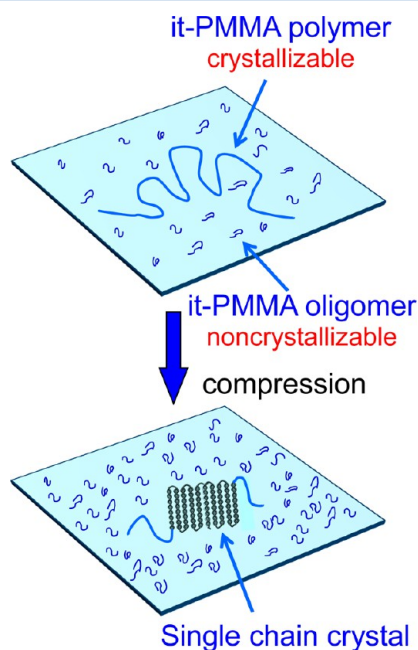


**Figure 1.** Schematic representation of crystallization of a single isolated it-PMMA chain solubilized in an it-PMMA oligomer monolayer upon compression.

of high-molecular-weight it-PMMA chains is solubilized in an it-PMMA oligomer monolayer, the molecular weight of which is too small to allow it to crystallize at the experimental temperature. If the mixed monolayer is then compressed up to the surface pressure of the crystalline transition, the high-molecular-weight it-PMMA chains ought to crystallize as single-chain crystals with the matrix monolayer staying amorphous. The it-PMMA 2D crystal is a 2D crystal and different from a conventional 3D crystal; however, its crystallographic parameters, the chain packing and the helical pitch of the chain, were in good agreement with the known values for the bulk crystal of it-PMMA.<sup>21,22</sup> Also, the crystal structures, such as the chain folding and tie chains, quite resembled those we expect for the bulk crystals.<sup>21</sup> Therefore, from the molecular images of the 2D crystals, we can expect new insights for the general crystallization mechanism.

As is shown later, the high-molecular-weight it-PMMA chains did successfully crystallize from amorphous isolated chains to single-chain crystals upon compression of the mixed monolayer, and the molecular images of the single-chain crystals were observed by AFM. Detailed AFM observations indicated that the crystalline nuclei preferentially formed at the ends of the chains, and their size was almost independent of the molecular weight of it-PMMA over a wide range. The crystallization of the single-chain crystals strongly depended on the compression rate.

## 2. EXPERIMENTAL METHODS

**2.1. Materials.** It-PMMA with a number-average molecular weight ( $M_n$ ), a polydispersity index ( $M_w/M_n$ ), and a *mm* content of  $2.90 \times 10^5$ , 1.13, and 98% (it-PMMA(290k)) and  $7.58 \times 10^5$ , 1.40, and 98% (it-PMMA(758k)) were prepared by the isotactic-specific anionic living polymerization of MMA in toluene at  $-78$  °C with *tert*-butylmagnesium bromide as an initiator.<sup>34</sup> The  $M_n$  and  $M_w/M_n$  values were measured by size exclusion chromatography (SEC) in chloroform using PMMA standards (Shodex, Tokyo, Japan) for the calibration. The tacticities were determined from the  $^1\text{H}$  NMR signals of the  $\alpha$ -methyl protons. An it-PMMA oligomer (it-PMMA(590):  $M_n$  = 590,  $M_w/M_n$  = 1.13) was prepared by the same anionic living polymerization system; the  $M_n$  and  $M_w/M_n$  were determined by NMR and SEC, respectively, while the *mm* content could not be precisely determined due to a highly split NMR spectrum of the oligomer. It-PMMA with a  $M_n$ , a  $M_w/M_n$ , and a *mm* content of  $1.76 \times 10^5$ , 1.21, and 97% (it-PMMA(176k)) and  $1.40 \times 10^6$ , 1.90, and 98% (it-PMMA(1400k)) were purchased from Polymer Source, Inc. (Montreal, Canada). Highly purified chloroform (Infinity Pure, Wako Chemicals, Osaka, Japan) was used as the solvent for the spreading solutions without further purification. Water was purified by a Milli-Q system and used as the subphase for the LB investigations.

**2.2. Surface Pressure–Area ( $\pi$ –*A*) Isotherm Measurements and Langmuir–Blodgett (LB) Film Preparations for AFM.** The  $\pi$ –*A* isotherms were measured as follows. An it-PMMA or mixture solution in chloroform having a concentration from  $6.2 \times 10^{-5}$  to  $1.2 \times 10^{-4}$  g/mL was spread on a water surface at 22 °C in a commercial LB trough with an area of  $37.5 \times 10 \text{ cm}^2$  and an effective moving barrier length of 10 cm (3-22YG3, USI, Fukuoka, Japan). The surface pressure was measured using filter paper as the Wilhelmy plate. The  $\pi$ –*A* isotherms were measured at a constant compression rate with a moving barrier speed of 0.5 mm/s. For AFM observation, an it-PMMA or mixture monolayer was first compressed at a moving barrier speed of 0.5 mm/s on a water surface at 22 °C or 0.01 mm/s at 6 °C, or 0.0004 mm/s at 6 °C to a specific surface pressure, and then deposited on a piece of freshly cleaved mica by pulling it out of the water at a rate of 4.2 mm/min, while compressing the monolayer at the constant pressure (the vertical dipping method). In order to save time, for the extremely slow compression rates of 0.01 and 0.0004 mm/s, monolayers were first compressed at 0.5 mm/s to 1 mN/m where no crystallization started and then the compression rate was reduced to 0.01 or 0.0004 mm/s. The compression of the monolayers in this way took about 10 min for 0.5 mm/s, 3 h for 0.01 mm/s, and 70 h for 0.0004 mm/s, respectively.

**2.3. AFM Observation and Analysis.** After the deposited monolayers were dried in vacuo, they were observed by a commercial AFM (NanoScope IIIa or IV/multimode AFM unit, Bruker AXS, Santa Barbara, CA, USA) with standard silicon cantilevers (NCH, Bruker AXS) in air at room temperature in the tapping mode. The typical settings of the AFM observations were as follows: target amplitude of 1.0–1.2 V, set point of 0.65–0.95 V, and scan rate of 2.0 Hz. The AFM images obtained are presented without any image processing except flattening. The thickness of lamella crystals was evaluated using 2D *Single Molecules* freeware by Y. Roiter and S. Minko, available for download at <http://people.clarkson.edu/~sminko>.



### 3. RESULTS AND DISCUSSION

**3.1.  $\pi$ -A Isotherms and AFM Images of Monolayers Composed of High-Molecular-Weight It-PMMA and It-PMMA Oligomer Mixtures.** Figure 2a shows  $\pi$ -A isotherms

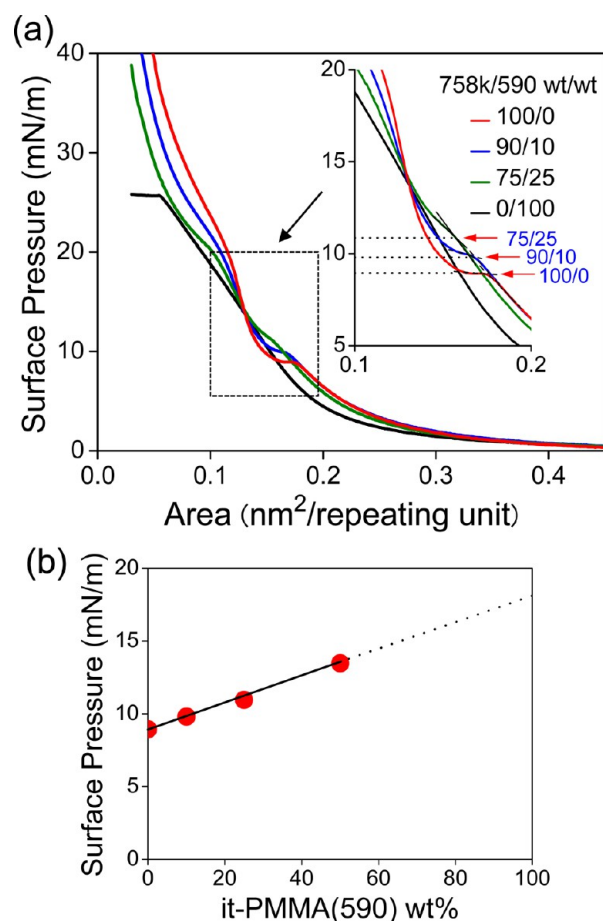
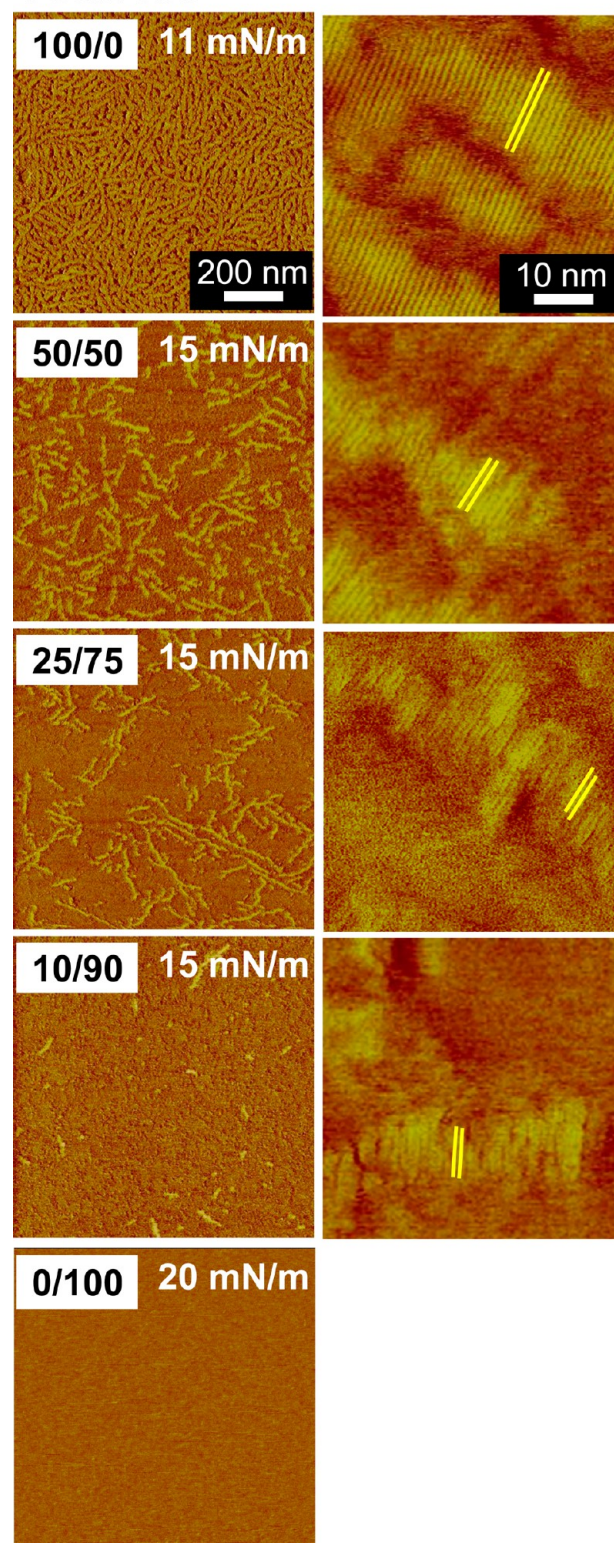


**Figure 2.** (a)  $\pi$ -A isotherms of monolayers of it-PMMA(758k), it-PMMA(590), and their mixtures on a water surface. As indicated in the magnified  $\pi$ -A isotherms, a plateau transition corresponding to crystallization of the it-PMMA(758k) increased with dilution by the oligomer. (b) Composition dependence of the  $\pi$  at the crystallization transition.

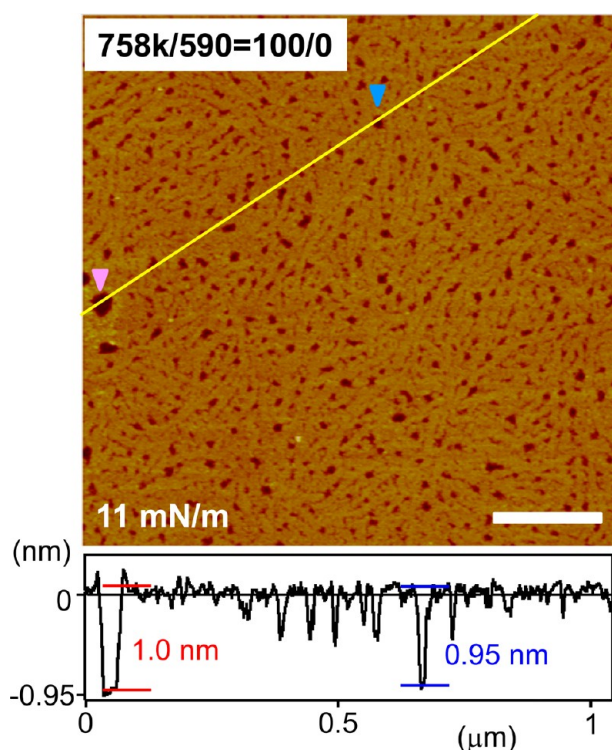
of it-PMMA(758 K), it-PMMA(590), and their mixtures on a water surface. It-PMMA(758k) has a plateau transition at around 9 mN/m, that corresponds to the crystallization into 2D folded-chain lamella crystals.<sup>21,35</sup> On the other hand, it-PMMA(590) shows no crystallization transition, indicating that it cannot crystallize due to its low molecular weight. The mixtures exhibit the crystallization transitions corresponding to their compositions; the  $\pi$  at the transition became higher with the addition of it-PMMA(590) (see red arrows in inset). Figure 2b shows the  $\pi$  at the plateau transition as a function of the composition. The increase of the  $\pi$  at the crystallization with the addition of it-PMMA(590) indicates the crystallization of it-PMMA(758k) was disturbed by the dilution with the oligomer.

Figure 3 shows AFM phase images of monolayers deposited on mica after compression at a rate of 0.5 mm/s up to the surface pressures indicated in the images. It-PMMA(758k) shows well-formed lamella crystals. Figure 4 shows a corresponding AFM height image of the monolayer along with the height profile. The thickness of the crystal from the

### 758k/590



**Figure 3.** AFM phase images of it-PMMA(758k)/it-PMMA(590) mixed monolayers deposited on mica at  $\pi$  sufficiently higher than the crystallization transitions; the  $\pi$  values are indicated in the images. The monolayers were compressed at a rate of 0.5 mm/s at a subphase temperature of 22 °C. The magnified images are shown in the left column, in which the yellow bars indicate an it-PMMA double-stranded helix packed in lamella crystals.



**Figure 4.** AFM height image of it-PMMA(758k) monolayer deposited on mica at 11 mN/m corresponding to the upper left phase image in Figure 3. The height profile along the yellow line is also shown. Scale bar = 200 nm.

mica surface was measured using holes indicated by pink and blue arrows and was found to be about 1.0 nm by AFM, which was in good agreement with that of a single crystalline plane of the it-PMMA (ca. 1.06 nm). In Figure 3, a magnified AFM image in the right column shows that helices are packed perpendicular to the long axis of the lamella (yellow lines) with a helix–helix distance of about 1.21 nm, similar to that reported previously.<sup>21,22</sup> Kusanagi and Tadokoro studied the crystal structure of uniaxially stretched it-PMMA strands by X-ray scattering, and analyzed it to be a crystal composed of double-stranded helices.<sup>36,37</sup> In their model, two 10/1 helices of it-PMMA chains (10 MMA units per turn) are intertwined to form a double helix, which packs in an orthorhombic crystal with a helix–helix distance of about 1.22 nm. The helix–helix distance observed in the AFM image (1.21 nm) was in good agreement with the double-stranded helix model, indicating the lamellae are composed of the double-stranded helix of it-PMMA chains. The average lamella thickness (along the helix axis) was 13.3 nm. The length of a double-stranded helix of it-PMMA(758k) is estimated to be  $1.59 \times 10^3$  nm, assuming a double-stranded helix is composed of two PMMA chains; thus, the average folding number of the double helix in the lamella was 119 ( $=1.59 \times 10^3$  nm/13.3 nm). The folding number is halved, if we assume that a double-stranded helix is composed of a single it-PMMA chain. With the dilution by the it-PMMA oligomer, the amount of the crystals was reduced (left column) and the lamellae structures became somewhat disturbed, but even at the most dilute composition, it-PMMA(758k)/it-PMMA(590) = 10/90 wt/wt, the helix packing in the lamella was still visible with a similar helix–helix distance ( $1.22 \pm 0.2$  nm) (right column, yellow lines). It-PMMA(590) did not crystallize even when compressed at 20 mN/m. In Figure 5, the

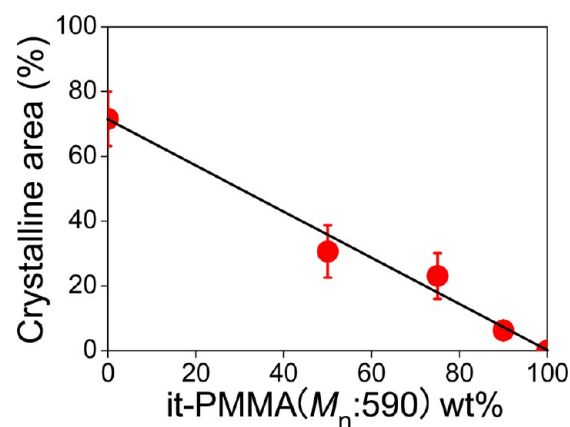


**Figure 5.** Composition dependence of the crystalline area ratio of the it-PMMA(758k)/it-PMMA(590) mixed monolayers shown in Figure 3.

area ratio occupied by the lamella crystals in Figure 3 is plotted against the composition. The crystalline area ratio dropped linearly with the reduction of the it-PMMA(758k) content, indicating that only the it-PMMA(758k) crystallized without induced crystallization of the it-PMMA(590). The distributions of the lamella thickness (along the helix axis) are shown in Figure 6 (red histogram). With the addition of it-PMMA(590), the average lamella thickness reduced from 13.3 nm (100/0 wt/wt) to 9.0 nm (10/90 wt/wt) (red circles), again indicating that the crystallization was disturbed by the dilution with the oligomer.

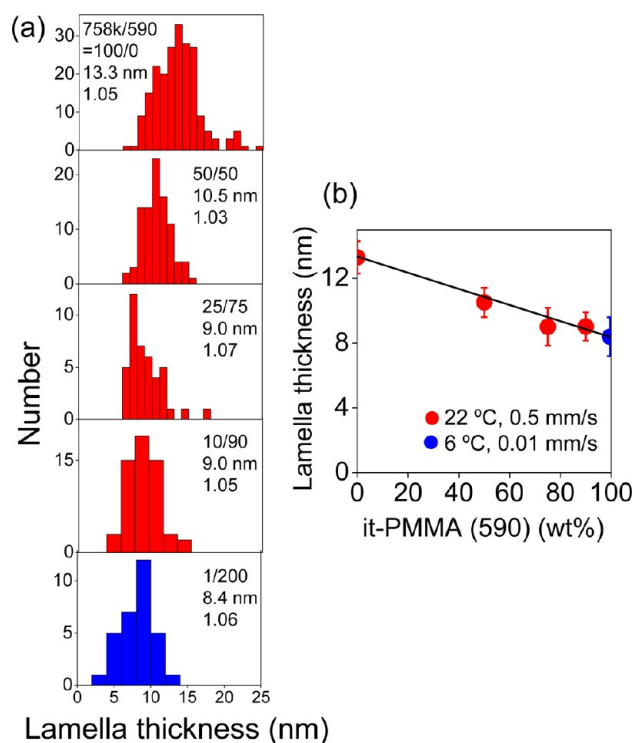


**Figure 6.** (a) Lamella thickness distribution of it-PMMA(758k)/it-PMMA(590) mixed monolayers similar to those in Figures 3 and 8. (b) Lamella thickness dependence on the composition. Data indicated in red were compressed at 0.5 mm/s at 22 °C, while data indicated in blue were compressed at 0.01 mm/s at 6 °C.



In Figure 7, it-PMMA(758k) was further diluted by the it-PMMA oligomer to compositions of it-PMMA(758k)/it-

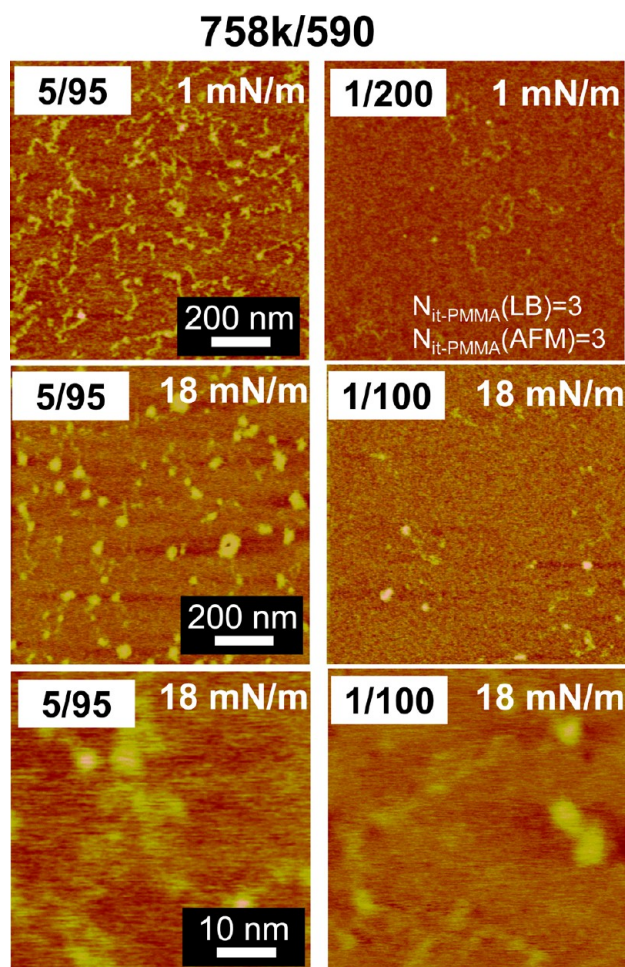


**Figure 7.** AFM height images of monolayers of it-PMMA(758k)/it-PMMA(590) mixtures (758k/590 = 5/95, 1/100, and 1/200 wt/wt) deposited on mica at 1 mN/m (first line) and 18 mN/m (second and third lines). The monolayers were compressed at a rate of 0.5 mm/s at a subphase temperature of 22 °C. Z range: 1.5 nm (first line), 2 nm (second and third lines).

PMMA(590) = 5/95, 1/100, and 1/200 wt/wt. For monolayers deposited at a low  $\pi$  of 1 mN/m, a crowded chain-like structure was visible at the 5/95 composition, while, with further dilution to the 1/200 composition, amorphous isolated PMMA chains solubilized in the matrix monolayer of the it-PMMA oligomer were clearly seen. The number of the isolated chains observed by AFM ( $N_{\text{it-PMMA}}(\text{AFM})$ ) was  $3/\mu\text{m}^2$  on average over wide areas, which was in good agreement with that expected from the deposition conditions of the LB monolayer ( $N_{\text{it-PMMA}}(\text{LB}) = 3/\mu\text{m}^2$ ), indicating the chains are it-PMMA(758k) chains solubilized in the oligomer monolayer. Previously, we reported that PMMA and poly(*n*-nonyl acrylate) (PNA) form a miscible monolayer, and if a small amount of PMMA was solubilized in a PNA monolayer, the PMMA isolated chains solubilized in the PNA monolayer could be clearly seen.<sup>26</sup> We believe that the contrast came from the different glass transition temperatures ( $T_g$ ) of the polymers. The PMMA chains with a high  $T_g$  of 105 °C were detected as higher than the matrix PNA with a low  $T_g$  (−89 °C) by AFM. In the present case, the high-molecular-weight it-PMMA(758k) was detected as higher than the

oligomer which is liquid at room temperature due to its low molecular weight. Upon compression up to 18 mN/m (second line), parts of the chains aggregated and formed globules. However, in high magnification (third line), we did not find any crystalline structures in the globules. We think that these globules probably formed by crystallization of the it-PMMA(758k), but at the higher dilution with the oligomer, they were not sufficiently stable to be observed by AFM under these conditions.

**3.2. Crystals Composed of Single Isolated Chains.** We tried various conditions to obtain a single chain crystal. The best result was attained by reducing the compression rate from 0.5 to 0.01 mm/s and lowering the subphase temperature from 22 to 6 °C. Figure 8 shows AFM height images of a monolayer of an it-PMMA(758k)/it-PMMA(590) = 1/200 mixture formed with these conditions. A monolayer deposited at 1 mN/m showed isolated it-PMMA chains solubilized in the oligomer monolayer (Figure 8a), but after compression at 18 mN/m, the chains converted to be aggregated (Figure 8b). A specific chain shown in Figure 8b crystallized at both ends (indicated by 1 and 3) and the middle of the chain (2), and these three small crystallites are connected by an amorphous chain, as schematically shown in Figure 8d. Figure 8c shows a magnified AFM phase image of the small crystallite 1 in Figure 8b; the clear folded-chain crystal image with chain packing indicates that the small crystallite is a well-characterized it-PMMA folded-chain crystal. The average number of chains in the AFM image ( $N_{\text{it-PMMA}}(\text{AFM}) = 7$ ) was in good agreement with that expected from the LB deposition conditions ( $N_{\text{it-PMMA}}(\text{LB}) = 6$ ), so we could conclude that this is a single chain crystal. In our best knowledge, we believe that this is the first molecular image of such a single chain crystal. The lamella thickness of the single chain crystal was added to Figure 6 (blue histogram and circle); the average lamella thickness was in line with those of other compositions, indicating that the lamella thickness of the single chain crystal is not extraordinarily different from that of the multimolecular crystals.

The single chain crystal crystallized at both ends and the middle of the chains. It is interesting to ask how the single chain crystallized. We know that it-PMMA forms the double-stranded-helix crystals. Therefore, we have to suppose that the crystallization proceeded as schematically shown in Figure 9. At the end of the chain, the chain intertwined to form a double-stranded helix, which immediately folded to form a folded chain crystal. At the middle of the chain, the chain also intertwined to form a double-stranded helix, which also immediately folded to form a folded-chain crystal.

**3.3. Crystal Behavior of Single Isolated Chains.** In our experimental method, we cannot directly see the crystallization process of single chains in real time. However, since there are many crystals at various crystalline stages in the AFM images, if we carefully analyze the crystalline structures, we may presume how they crystallized. Figure 10 summarizes various crystalline structures of it-PMMA(758k) single chain crystals. The AFM images show chains crystallized at one end (upper image), at both ends (middle image), and at five points, both ends and three in the middle of the chain, like a necklace (lower image). The 43 single chain crystals are classified in a table based on the number of crystallites in a chain, and the positions of them are marked by red circles. The three chains were classified as indicated by arrows. Close inspection indicates that (1) all single chain crystals crystallized at least at one end of the chain (blue line), (2) then after one end of the chain crystallized, the

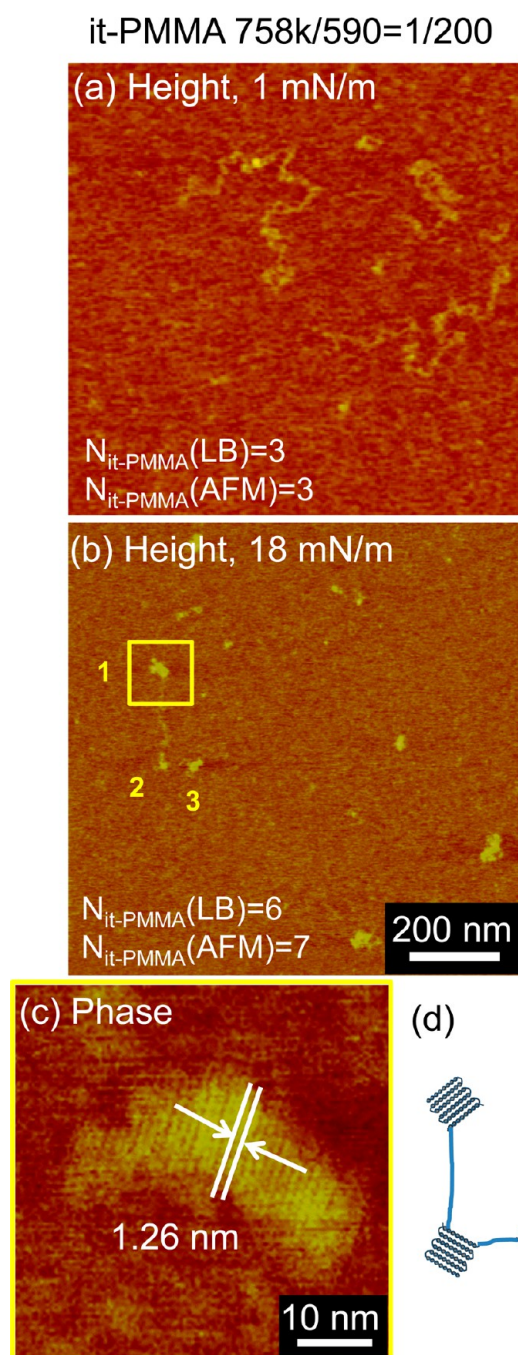


**Figure 8.** (a, b) AFM height images of it-PMMA(758k)/it-PMMA(590) mixed monolayers (758k/590 = 1/200 wt/wt) deposited on mica at (a) 1 mN/m and (b) 18 mN/m, respectively. (c) Magnified AFM phase image corresponding to a yellow square in part b. (d) Schematic representation of a single chain crystallized at both ends and the middle of a chain shown in part b. The monolayers were compressed at a rate of 0.01 mm/s at a subphase temperature of 6 °C. Z range: (a) 1.5 nm, (b) 2.0 nm.

other end of the chain crystallized (yellow line), and (3) after both ends crystallized, the middle of the chain crystallized accordingly (from the third to fifth lines). Therefore, we conclude that the single chain is more easily crystallized at the end of the chain than at the middle of the chain.

The end of a chain is believed to be excluded from the crystals, because they form crystalline defects.<sup>1–3</sup> In that case, why did the single chain crystallize preferentially at the end of

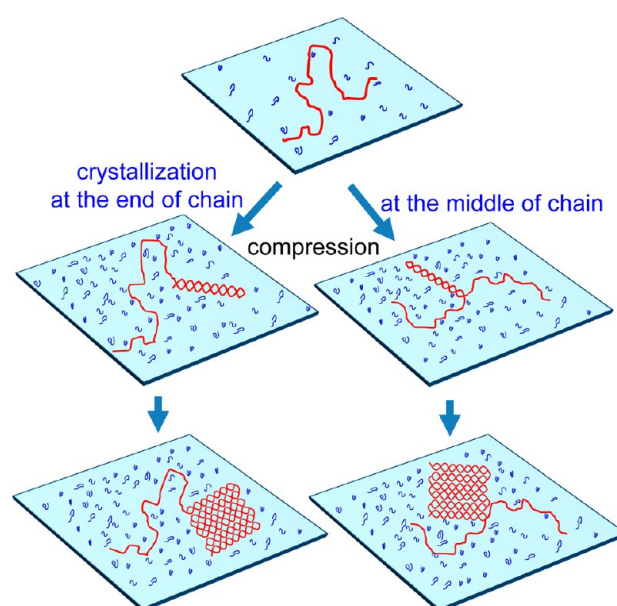


**Figure 9.** Schematic representation of a plausible crystallization mechanism of a single chain at an end and in the middle of the chain.

the chain in the present study? The reason is not presently clear; however, we think there are three possible reasons which rationalize the present results. The first is the higher mobility of the chain end than the middle of the chain. At the high surface pressure at the crystallization, the matrix monolayer is solidified. In order to crystallize, the chain needs to pull the rest of the chain from the matrix. This should be easier at the end of the chain than the middle of the chain. As a result, the end of the chain should be more easily crystallized than the middle of the chain. The second point is that only the chain end should be a crystal defect. The chain parts near the end, but spaced from the end by a few lamella thicknesses (about a few tens of nm), will not be defects, and hence are expected to be more easily crystallized with a higher mobility than the middle of chain as mentioned above. If only a short chain end is excluded from the crystals, it may be difficult to recognize by AFM. Moreover, after the crystallization, the excluded short chain may be adsorbed at the crystalline surface and be induced to crystallize, and as a result, the chain may look like it has crystallized at the end of the chain. The third explanation is that the it-PMMA crystal is a double-stranded-helix crystal. The chain should pull the rest of the chain from the matrix and intertwine it to form a crystallite. This is, again, easier at the end of the chain than the middle of the chain.

Muthukumar and co-workers studied the crystallization behavior of a single chain in a solution by Langevin dynamics simulations and theoretical models.<sup>38</sup> Their simulation results resembled our observations quite closely. The simulation indicated that, in the early stage, a single chain formed several “baby nuclei” along the chain with a relatively constant separation. The “baby nuclei” were connected by the amorphous flexible chain. As time proceeded, the amorphous chain became tight by being reeled into the “baby nuclei” to fuel their growth. Further, the “baby nuclei” competed with each other to grow, and as a result, some nuclei grew to be folded-chain crystals but others unfolded and disappeared. The necklace-like structures connected with tight chains observed in our work (Figures 8 and 10) are quite similar to their simulation results. The distance between the “baby nuclei” is



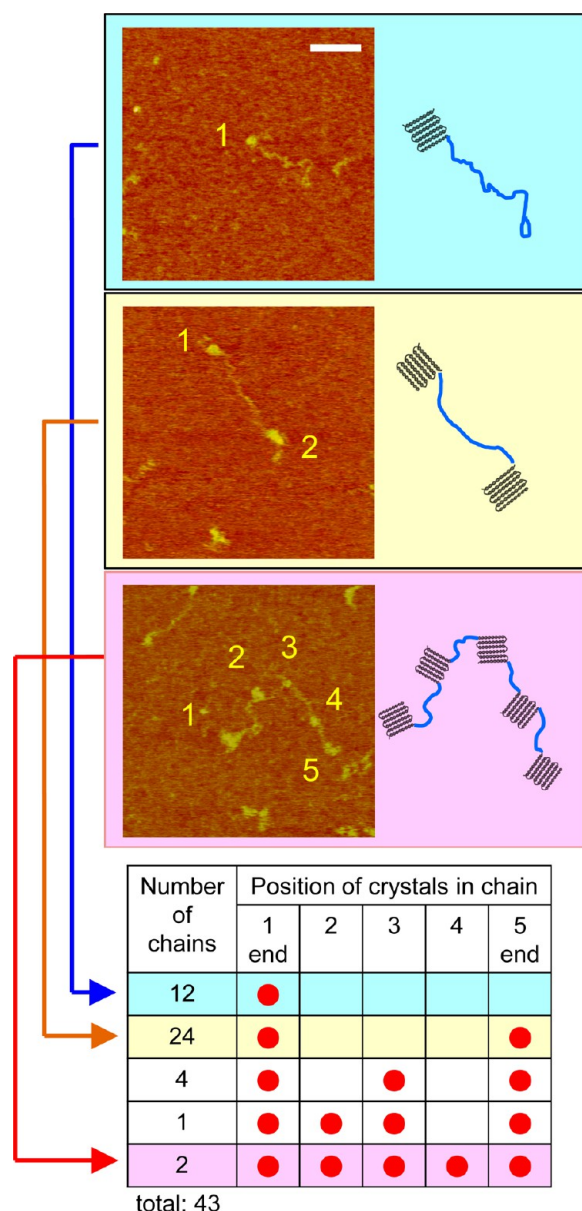


**Figure 10.** (Upper images) AFM height images of various crystalline structures of single it-PMMA(758k) chains. It-PMMA(758k)/it-PMMA(590) (1/200) mixed monolayers were compressed at 0.01 mm/s at 6 °C. Scale bar = 100 nm. (Lower table) 43 single-chain crystals were classified by the number and the position of small crystallites formed in the chain. Z range: 2.0 nm.

relatively constant during the initial stage of the crystallization and, based on their theory, is a function of the quench depth for the crystallization. In our experiment, the distance between the small crystallites may depend on the  $\pi$  value and the compression rate, but this was not systematically studied in the present study.

**3.4. Molecular Weight Dependence of Single Chain Crystals.** Figure 11 shows single chain crystals prepared from various molecular weight it-PMMA with  $M_n$  values from 176k to 1400k. As schematically shown in the left column, the chains contain one (76k and 290k), three (758k), and six crystallites (1400k) in the chain, respectively. The magnified AFM phase images of the crystallite (middle column) corresponding to yellow squares in the left AFM images clearly show the it-PMMA folded-chain-crystal structures with the chain packing.

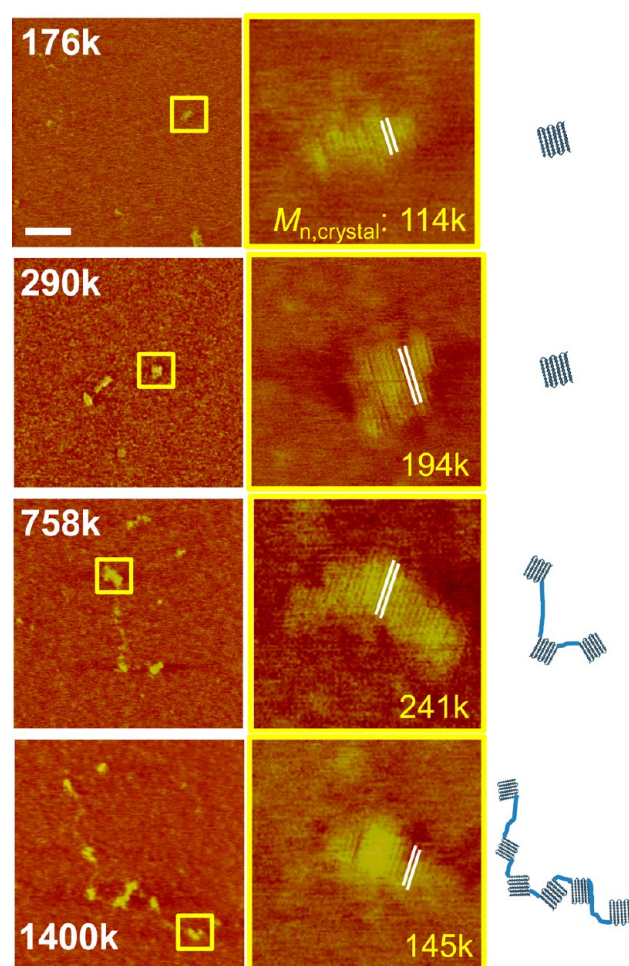


**Figure 11.** (Left column) AFM height images of single-chain crystals formed from various molecular weight chains from 176k to 1400k. Z range: 2.0 nm. Scale bar = 100 nm. (Center column) Magnified AFM phase images corresponding to yellow squares in the left images. The white bars indicate an it-PMMA double-stranded helix packed in the crystallites.  $M_n$  values estimated from the molecular image of the small crystallite are also shown. (Right column) Schematic representation of the single-chain crystals shown in the AFM height images. It-PMMA(176k–1400k)/it-PMMA(590) (1/200) mixed monolayers were compressed at 0.01 mm/s at 6 °C.

On the basis of the molecular images of the crystallite, the  $M_n$  values of each crystallite were evaluated and were found to range from 114k to 241k, as indicated in the images. Note that, although the  $M_n$  of the it-PMMA varied by a factor of 10 (176k–1400k), the  $M_n$  of the small crystallites was almost the same (114k–241k). The size of the small crystallite is almost independent of the  $M_n$  of the polymers. We do not think that the small crystallite in the chain is a crystalline nuclei itself; however, we could expect that it reflects the structures of the crystalline nuclei. Therefore, we may assume that the size of crystalline nuclei is independent of the molecular weight of the polymers.

**3.5. Single Chain Crystals Compressed at an Extremely Slow Rate.** As shown in Figure 11, the low-molecular-weight it-PMMA(176k, 290k) crystallized as whole chains, while, on the other hand, the high-molecular-weight it-PMMA(758k, 1400k) only crystallized in parts of the chains. In the present system, the crystallization of the mixed monolayer upon compression is a competition. The compression

promotes the crystallization of the it-PMMA polymer, but on the other hand, it solidifies the matrix monolayer to reduce the mobility of the it-PMMA polymer and, as a result, prevents the crystallization of the it-PMMA polymer. At a certain compression rate, the crystallization was prevented more significantly for the higher-molecular-weight it-PMMA. We expected, if the mixed monolayer is compressed at an extremely slow rate, even the high-molecular-weight it-PMMA polymer may crystallize more perfectly. Figure 12 shows AFM phase images of a monolayer of an it-PMMA(1400k)/it-PMMA(590) (1/200) mixture compressed at an extremely slow rate of 0.0004 mm/s at a subphase temperature of 6 °C. The compression rate was 25 times slower than the normal condition (0.01 mm/s), and it took 70 h to compress the monolayer (vs 3 h at 0.01 mm/s). As shown in Figure 12, the whole chains crystallized. In the magnified images (Figure 12a',b'), the helix packing in the crystals are clearly seen. The molecular weight of the crystals based on the molecular images was  $1.36 \times 10^6$  (upper) and  $1.05 \times 10^6$  (bottom), respectively. Taking into account the molecular weight distribution, the values agree well with crystallization of the whole chains. The upper crystal seems to be composed of several small crystals; however, as is interesting, the directions of the chain packed in the crystals look almost identical, indicating that the small crystals formed during the compression gathered to align their chain directions. The lower crystal looks like a single crystal; the chain direction is again almost identical throughout the crystal. However, the lamella thickness varied significantly, which may indicate that the crystal formed by alignment of small crystals.

The sizes of the crystals were significantly dependent on the compression rates. As shown in Figures 7 and 8, we could not observe a single-chain crystal at a compression rate of 0.5 mm/s but successfully visualized it at 0.01 mm/s. Taking into account the large compression-rate dependence of the crystal size shown here, we now think that a single-chain crystal formed at a compression rate of 0.5 mm/s was too small to stay stable. Strictly speaking, the lower subphase temperature (6 °C for 0.01 mm/s) may also have an additional effect on the stability of the crystals.

#### 4. CONCLUSION

We have, for the first time, successfully visualized the crystallization behavior of a single isolated polymer chain by compressing a mixed monolayer composed of a small amount of a high-molecular-weight it-PMMA solubilized in an it-PMMA oligomer monolayer, whose molecular weight is too small to crystallize under the experimental conditions. The single-chain crystals were observed by AFM at the molecular level. The observation indicated that the crystalline nuclei formed preferentially at the end of the chain rather than the middle of the chain, and the size of the crystalline nuclei is almost independent of the molecular weight of the polymer. The crystallization of the single chain in the mixed monolayer was strongly dependent on the compression rate; crystallization proceeded throughout the chain at a lower compression rate.

Finally, we note that the new methodology we used here in order to observe the crystallization of a single chain may also be applicable to visualize other self-assembly processes of a single chain. In recent years, single-chain technology has attracted intense interest.<sup>39</sup> Conventional polymers are used as bulk materials composed of numerous molecules. In contrast, biomacromolecules, such as enzymes, antibodies, and proteins,

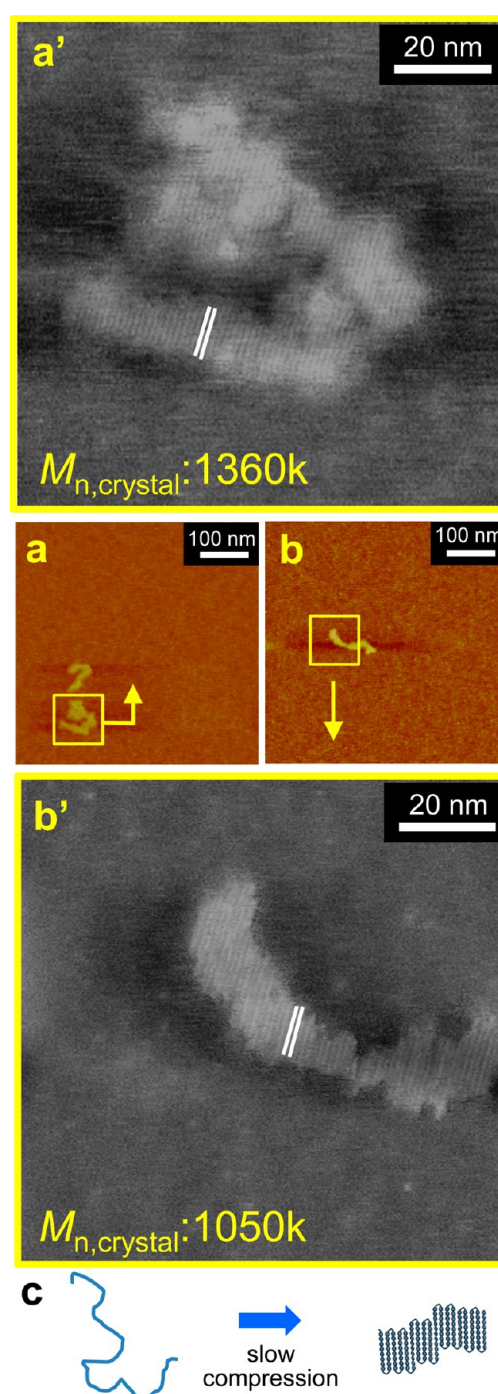


**Figure 12.** (a, b) AFM phase images of a monolayer of it-PMMA(1400k)/it-PMMA(590) (1/200 wt/wt) deposited on mica, after being compressed to 18 mN/m at a rate of 0.0004 mm/s and a subphase temperature of 6 °C. (a', b') Magnified AFM phase images corresponding to areas indicated by yellow squares in the images in parts a and b. The white bars indicate an it-PMMA double-stranded helix packed in the crystals. Estimated  $M_n$  of the crystals are indicated in the images. (c) A schematic representation of perfect crystallization of a single chain at a slow compression rate is also shown.

form sophisticated structures composed of a single or few molecules, which play important roles in biology. In order to mimic these biological functions, researchers have started trying to molecularly design single chains and self-assemble them to be unimolecular particles with controlled structures in order to use them as highly functionalized materials.<sup>40–42</sup> The present



methodology that uses a mixed monolayer may provide a possible method to visualize these self-assembly processes of single chains at a molecular level.

## AUTHOR INFORMATION

### Corresponding Author

\*E-mail: kumaki@yz.yamagata-u.ac.jp.

### Present Addresses

<sup>§</sup>(For T.A.) Engineering Research Department, Corporate Technology Office, NOK Corporation, 4-3-1, Tsujidoshinmachi, Fujisawa, Kanagawa 251-0042, Japan.

<sup>||</sup>(For T.K.) Iyoda Supra-Integrated Material Project, ERATO, Japan Science and Technology Agency, and Frontier Research Center, Tokyo Institute of Technology, 4259-S2-3 Nagatsuta-Cho, Midori-Ku, Yokohama, Kanagawa 226-8503, Japan.

### Notes

The authors declare no competing financial interest.

## ACKNOWLEDGMENTS

This work was supported by JSPS KAKENHI Grant Numbers 24655091, 24350113, 25107706, and 26620092.

## REFERENCES

- (1) Wunderlich, B. *Macromolecular Physics*; Academic: New York, 1976; Vols. 1–3.
- (2) Organization of Macromolecules in the Condensed Phase. *Faraday Discuss. Chem. Soc.* **1979**, 68, 7–516.
- (3) Mandelkern, L. *Crystallization of Polymers*; Cambridge University Press: Edinburgh, Scotland, 2002; Vols. 1 and 2.
- (4) Sommer, J.-U.; Reiter, G., Eds. *Polymer Crystallization*; Springer: Berlin, 2003.
- (5) Strobl, G. Crystallization and Melting of Bulk Polymers: New Observations, Conclusions and a Thermodynamic Scheme. *Prog. Polym. Sci.* **2006**, 31, 398–442.
- (6) Cao, J.; Gu, F.; Liu, Y.; Bi, S.; Bu, H.; Zhang, Z. Single-Chain Single Crystals. *Macromol. Symp.* **1997**, 124, 89–109.
- (7) Bu, H.; Gu, F.; Bao, L.; Chen, M. Influence of Entanglements on Crystallization of Macromolecules. *Macromolecules* **1998**, 31, 7108–7110.
- (8) Magonov, S. N.; Whangbo, M.-H. *Surface Analysis with STM and AFM*; VCH: Weinheim, Germany, 1996.
- (9) Magonov, S. N. Atomic force Microscopy in Analysis of Polymers. In *Encyclopedia of Analytical Chemistry*; Meyers, R. A., Ed.; John Wiley & Sons: Chichester, U.K., 2000; pp 7432–7491.
- (10) Schönherr, H.; Vancso, G. V. *Scanning Force Microscopy of Polymers*; Springer: Heidelberg, Germany, 2010.
- (11) Tsukruk, V. V.; Singamaneni, S. *Scanning Probe Microscopy of Soft Matter: Fundamentals and Practices*; Wiley-VCH: Weinheim, Germany, 2012.
- (12) Sheiko, S. S.; Möller, M. Visualization of Molecules – A First Step to Manipulation and Controlled Response. *Chem. Rev.* **2001**, 101, 4099–4123.
- (13) Samorì, P.; Surin, M.; Palermo, V.; Lazzaroni, R.; Leclère, P. Functional Polymers: Scanning Force Microscopy Insights. *Phys. Chem. Chem. Phys.* **2006**, 8, 3927–3938.
- (14) Rabe, J. P. Molecular Workbench for Imaging and Manipulation of Single Macromolecules and Their Complexes with the Scanning Force Microscope. *Top. Curr. Chem.* **2008**, 285, 77–102.
- (15) Kumaki, J.; Sakurai, S.-i.; Yashima, E. Visualization of Synthetic Helical Polymers by High-Resolution Atomic Force Microscopy. *Chem. Soc. Rev.* **2009**, 38, 737–746.
- (16) Hobbs, J. K.; Farrance, O. E.; Kailas, L. How Atomic Force Microscopy Has Contributed to Our Understanding of Polymer Crystallization. *Polymer* **2009**, 50, 4281–4292.
- (17) Gallyamov, M. O. Scanning Force Microscopy as Applied to Conformational Studies in Macromolecular Research. *Macromol. Rapid Commun.* **2011**, 32, 1210–1246.
- (18) Kumaki, J.; Nishikawa, Y.; Hashimoto, T. Visualization of Single Chain Conformations of a Synthetic Polymer with Atomic Force Microscopy. *J. Am. Chem. Soc.* **1996**, 118, 3321–3322.
- (19) Kumaki, J.; Hashimoto, T. Conformational Change in Isolated Single Synthetic Polymer Chain on Mica Surface Observed by Atomic Force Microscopy. *J. Am. Chem. Soc.* **2003**, 125, 4907–4917.
- (20) Kumaki, J.; Kawauchi, T.; Yashima, E. “Reptational” Movements of Single Synthetic Polymer Chains on Substrate Observed by In-situ Atomic Force Microscopy. *Macromolecules* **2006**, 39, 1209–1215.
- (21) Kumaki, J.; Kawauchi, T.; Yashima, E. Two-Dimensional Folded Chain Crystals of a Synthetic Polymer in a Langmuir-Blodgett Film. *J. Am. Chem. Soc.* **2005**, 127, 5788–5789.
- (22) Takanashi, Y.; Kumaki, J. Significant Melting Point Depression of Two-Dimensional Folded-Chain Crystals of Isotactic Poly(methyl methacrylate)s Observed by High-Resolution In-Situ Atomic Force Microscopy. *J. Phys. Chem. B* **2013**, 117, 5594–2605.
- (23) Kumaki, J.; Kawauchi, T.; Okoshi, K.; Kusanagi, H.; Yashima, E. Supramolecular Helical Structure of the Stereocomplex Composed of Complementary Isotactic and Syndiotactic Poly(methyl methacrylate)s as Revealed by Atomic Force Microscopy. *Angew. Chem., Int. Ed.* **2007**, 46, 5348–5351.
- (24) Kumaki, J.; Kawauchi, T.; Ute, K.; Kitayama, T.; Yashima, E. Molecular Weight Recognition in the Multiple-Stranded Helix of a Synthetic Polymer without Specific Monomer-Monomer Interaction. *J. Am. Chem. Soc.* **2008**, 130, 6373–6380.
- (25) Kumaki, J.; Kajitani, T.; Nagai, K.; Okoshi, K.; Yashima, E. Visualization of Polymer Chain Conformations in Amorphous Polyisocyanide Langmuir-Blodgett Films by Atomic Force Microscopy. *J. Am. Chem. Soc.* **2010**, 132, 5604–5606.
- (26) Sugihara, K.; Kumaki, J. Visualization of Two-Dimensional Single Chain Conformations Solubilized in Miscible Polymer Blend Monolayer by Atomic Force Microscopy. *J. Phys. Chem. B* **2012**, 116, 6561–6568.
- (27) Sakurai, S.-i.; Okoshi, K.; Kumaki, J.; Yashima, E. Two-Dimensional Hierarchical Self-Assembly of One-Handed Helical Polymers on Graphite. *Angew. Chem., Int. Ed.* **2006**, 45, 1245–1248.
- (28) Sakurai, S.-i.; Okoshi, K.; Kumaki, J.; Yashima, E. Two-Dimensional Surface Chirality Control by Solvent-Induced Helicity Inversion of a Helical Polyacetylene on Graphite. *J. Am. Chem. Soc.* **2006**, 128, 5650–5651.
- (29) Sakurai, S.-i.; Ohsawa, S.; Nagai, K.; Okoshi, K.; Kumaki, J.; Yashima, E. Two-Dimensional Helix-Bundle Formation of a Dynamic Helical Poly(phenylacetylene) with Achiral Pendant Groups on Graphite. *Angew. Chem., Int. Ed.* **2007**, 46, 7605–7608.
- (30) Kajitani, T.; Okoshi, K.; Sakurai, S.-i.; Kumaki, J.; Yashima, E. Helix-Sense Controlled Polymerization of a Single Phenyl Isocyanide Enantiomer Leading to Diastereomeric Helical Polyisocyanides with Opposite Helix-Sense and Cholesteric Liquid Crystals with Opposite Twist-Sense. *J. Am. Chem. Soc.* **2006**, 128, 708–709.
- (31) Onouchi, H.; Okoshi, K.; Kajitani, T.; Sakurai, S.-i.; Nagai, K.; Kumaki, J.; Onitsuka, K.; Yashima, E. Two- and Three-Dimensional Smectic Ordering of Single-Handed Helical Polymers. *J. Am. Chem. Soc.* **2008**, 130, 229–236.
- (32) Maeda, T.; Furusho, Y.; Sakurai, S.-i.; Kumaki, J.; Okoshi, K.; Yashima, E. Double-Stranded Helical Polymers Consisting of Complementary Homopolymers. *J. Am. Chem. Soc.* **2008**, 130, 7938–7945.
- (33) Ohsawa, S.; Sakurai, S.-i.; Nagai, K.; Banno, M.; Maeda, K.; Kumaki, J.; Yashima, E. Hierarchical Amplification of Macromolecular Helicity of Dynamic Helical Poly(phenylacetylene)s Composed of Chiral and Achiral Phenylacetylenes in Dilute Solution, Liquid Crystal, and Two-Dimensional Crystal. *J. Am. Chem. Soc.* **2011**, 133, 108–114.
- (34) Hatada, K.; Ute, K.; Tanaka, K.; Okamoto, Y.; Kitayama, T. Living and Highly Isotactic Polymerization of Methyl Methacrylate by  $t\text{-C}_4\text{H}_9\text{MgBr}$  in Toluene. *Polym. J.* **1986**, 18, 1037–1047.

- (35) Brinkhuis, R. H. G.; Shouten, A. J. Thin-Film Behavior of Poly(methyl methacrylates). 1. Monolayers at the Air-Water Interface. *Macromolecules* **1991**, *24*, 1487–1495.
- (36) Kusanagi, H.; Tadokoro, H.; Chatani, Y. Double Strand Helix of Isotactic Poly(methyl methacrylate). *Macromolecules* **1976**, *9*, 531–532.
- (37) Kusanagi, H.; Chatani, Y.; Tadokoro, H. The Crystal Structure of Isotactic Poly(methyl methacrylate): Packing-Mode of Double Stranded Helices. *Polymer* **1994**, *35*, 2028–2039.
- (38) Muthukumar, M. Molecular Modelling of Nucleation in Polymers. *Philos. Trans. R. Soc. London, Ser. A* **2003**, *361*, 539–556.
- (39) Ouchi, M.; Badi, N.; Lutz, J.-F.; Sawamoto, M. Single-Chain Technology Using Discrete Synthetic Macromolecules. *Nat. Chem.* **2011**, *3*, 917–914.
- (40) Harth, E.; Van Horn, B.; Lee, V. Y.; Germack, D. S.; Gonzales, C. P.; Miller, R. D.; Hawker, C. J. A Facile Approach to Architecturally Defined Nanoparticles via Intramolecular Chain Collapse. *J. Am. Chem. Soc.* **2002**, *124*, 8653–8660.
- (41) Foster, E. J.; Berda, E. B.; Meijer, E. W. Metastable Supramolecular Polymer Nanoparticles via Intramolecular Collapse of Single Polymer Chains. *J. Am. Chem. Soc.* **2009**, *131*, 6964–6966.
- (42) Mes, T.; van der Weegen, R.; Palmans, A. R. A.; Meijer, E. W. Single-Chain Polymeric Nanoparticles by Stepwise Folding. *Angew. Chem., Int. Ed.* **2011**, *50*, 5085–5089.